J. exp. Biol. 142, 49–85 (1989)
Printed in Great Britain © *The Company of Biologists Limited 1989*

THE KINEMATICS AND AERODYNAMICS OF THE FREE FLIGHT OF SOME DIPTERA

BY A. ROLAND ENNOS*

Department of Biological Sciences, Hatherly Laboratories, University of Exeter, Prince of Wales Road, Exeter EX4 4PS

Accepted 26 September 1988

Summary

Seven representative species of the order Diptera were filmed in free flight using high-speed cinematography. Insects were killed after filming, and morphological measurements were made in the manner of Ellington (1984*b*).

The detailed kinematics of selected sequences were then found using frame-by-frame digitization, followed by computer reconstruction of the third dimension. Kinematics were qualitatively similar to those observed by Ellington (1984*c*), though in three species the wings often underwent ventral flexion near the base at the end of the downstroke.

For aerodynamic analysis of hovering flight, modified forms of the equations of Ellington (1984*e*,*f*) were used. Forward flight was analysed by a novel method, which assumes that an equal but opposite circulation is built up for each half-stroke and allows linear equations to be used.

The lift coefficients calculated for hovering were commonly well above those possible by quasi-steady mechanisms, but rotational coefficients were within those that could be achieved by the unsteady lift mechanisms: clap-and-fling (Weis-Fogh, 1973) and flex (Ellington, 1984*d*). The lift and rotational coefficients of the two half-strokes were often unequal.

In forward flight, the equal circulation assumption often led to an incorrect estimation of the aerodynamic force vector, showing that the circulations during the two half-strokes were unequal.

It is suggested that flies manoeuvre largely by altering the unsteady circulations produced at stroke reversal *via* alterations in the speed and timing of wing rotation. The differences in the mechanisms used by different fly species are related to their flight behaviour in the field.

Introduction

This paper is concerned with the kinematics and aerodynamics of the flight of

* Present address: Department of Biological Science, University of York, Heslington, York, YO1 5DD.

Key words: Diptera, flight, kinematics, aerodynamics.

selected species of Diptera, and with the methods they use to keep themselves aloft, propel themselves through the air and manoeuvre.

In recent years, the study of these aspects of insect flight has been revolutionized by the practical and theoretical advances of Weis-Fogh (1972, 1973), Lighthill (1973) and Ellington (1978, 1980; summarized in Ellington, 1984*a–f*). It is now possible to analyse the kinematics of insects in free flight and to test whether the aerodynamic forces produced by the wings can be explained using conventional aerodynamic theory. These techniques have led to an increasing awareness of the importance of unsteady effects in insect flight, and to greater understanding of how unsteady forces may be generated.

This paper summarizes these earlier studies and uses the results and speculations from them to help interpret the quantitative information on the kinematics of flight which was obtained from my films. Together with qualitative information from film and from field observations, a broad picture of the flight adaptations of the group can then be built up.

Theoretical basis of free-flight studies

Testing the quasi-steady assumption

In quasi-steady theory the aerodynamic effects of wing motion are calculated by assuming that the aerodynamic forces produced by each element of the wing are identical to those that would be produced by such elements travelling at the same *steady* velocity and angle of attack. Each spanwise element would produce a lift force per unit length (L′) at right angles to its velocity (Osborne, 1951):

$$L' = \rho c U^2 C_L/2,$$

and would experience drag:

$$D' = \rho c U^2 C_D/2,$$

where ρ is the density of air, c is the chord length, U is the velocity and C_L and C_D are the lift and drag coefficients, respectively, which can be found by testing real aerofoils at the correct Reynolds number. Alternatively, the lift and drag coefficients can be found for infinitely long aerofoils; the relative velocity of the wing is then found by adding its flapping velocity and a vector of the wake-induced velocity, calculated using Rankine–Froude propeller theory.

The method usually used to test whether quasi-steady effects may explain the observed balance of forces is to calculate the resulting mean values of the force coefficients $\bar{C}_L$ and $\bar{C}_D$. The quasi-steady assumption may be rejected in two cases: (i) if the value of $\bar{C}_L$ required is higher than the maximum that can be obtained from wings in a steady flow at the same Reynolds number; (ii) if the force vector calculated by the quasi-steady assumption is not in the same direction as the force vector inferred from the body motion.

The results of previous studies

Hovering is the most easily analysed mode of flight in insects, since there is no body motion to add to the flapping velocity, and the induced velocity is relatively easy to calculate. The resultant force must be vertical and must balance the weight of the insect. With no forward velocity of the body to be added, the wings show their greatest changes in direction of motion and rotate markedly in pitch. It is therefore the case in which unsteady effects are most likely to be important. For these reasons hovering has been the best studied flight mode in insects (Weis-Fogh, 1972, 1973; R. Å. Norberg, 1975; Ellington, 1984*a–f*). Two main kinematic patterns of hovering were identified by Weis-Fogh on the basis of the orientation of the stroke plane, which could be either horizontal or inclined away from this plane. Ellington (1980) identified a third kinematic pattern in the butterfly *Pieris brassicae*, with a vertical stroke plane. This pattern, however, was not observed in any of my films and will not be discussed.

Forward flight is more complex and a complete analysis has only very recently been attempted (Dudley, 1987). The stroke plane of animals in forward flight is generally inclined forwards, like the rotor of a helicopter, and the angle of inclination tends to rise with forward speed (Vogel, 1966; David, 1978).

Hovering with a horizontal stroke plane

In the most common form of hovering in insects the wings move along an approximately horizontal stroke plane with approximately equal angles of attack on the downstroke and upstroke. The force vector inferred from the use of the quasi-steady assumption is therefore vertical, which is in agreement with the balance of forces. There is less agreement about the magnitude of the lift coefficients needed. Weis-Fogh calculated lift coefficients of 0·6–1·3 for the dipterans in his study, just within the capabilities of low Reynolds number aerofoils, but in Ellington's more accurate study the mean lift coefficients calculated for two of the insects, a ladybird, *Coccinella 7-punctata*, and a crane fly, *Tipula obsoleta*, 1·71 and 1·24, respectively, were above that possible for quasi-steady aerofoils. Since these insects had kinematics which were qualitatively indistinguishable from the other insects in his study, he tentatively rejected the quasi-steady mechanism for all of them, including *Eristalis tenax*.

Hovering with an inclined stroke plane

Hoverflies, some dragonflies and some of the smaller birds and bats hover with a stroke plane inclined to the horizontal. The pied flycatcher *Ficedula hypoleuca* and a small bat *Plecotus auritus* were observed to fold their wings on the upstroke (U. M. Norberg, 1975, 1976) so that little force was produced. In insects, however, the wing cannot fold and Ellington (1984*c*) found that the angles of attack were similar for both strokes in the hoverfly *Episyrphus balteatus*. In this case, the quasi-steady estimate of force was at right angles to the stroke plane, about 30° forward of vertical; however, since the insect was hovering, the wings must have been

producing a vertical force. Lift must have been produced mainly on the downstroke, as was more clearly the case with Norberg's bird and bat. In all these cases the values of the average lift coefficient for the downstroke exceeded 3, easily greater than the limit for aerofoils. The quasi-steady assumption should be rejected on both counts. It is clear that unsteady effects must be important during inclined stroke plane hovering.

Forward flight

In his study of the forward flight of bumblebees, *Bombus terrestris*, and hoverflies, *Eristalis tenax*, Dudley (1987) showed that to balance their weight, average lift coefficients higher than 1 were needed, whereas experimental tests showed that the lift coefficients that the wings could produce were all below 1. Clearly, unsteady effects must also be important in forward flight.

Unsteady mechanisms of lift generation

Lift generation by a wing section relies on the movement of a bound circulation through the air. In steady flow past an aerofoil the circulation is itself created by the translation of the asymmetrical aerofoil section. Since lift forces are proportional to the circulation multiplied by the relative velocity, lift is proportional to the second power of the velocity. Several chord lengths of translation are necessary before lift reaches its steady-state value, a phenomenon known as the Wagner effect (Wagner, 1925). This would seem to prevent the maximum values of lift predicted by quasi-steady theory from being reached in typical insect flight. Unsteady mechanisms of lift production may explain how large (but ultimately unstable) circulations may be rapidly built up without translation of the wing. Such circulations may stay attached to the wing for several chord lengths of translation.

Several unsteady mechanisms of lift generation have been suggested to operate in insects.

The clap-and-fling mechanism

The best understood and experimentally verified unsteady mechanism is clap-and-fling, first described and analysed by Weis-Fogh (1973) and Lighthill (1973) (Fig. 1A). If two wings are clapped together at the end of a stroke the circulation around each is immediately destroyed. If the wings are then flung open, leading edge first, air will rush into the vacuum created, resulting in a circulation being built up around each wing. At low Reynolds numbers this circulation may become attached to the wing. An even more effective means of creating circulation is to peel the wings apart (Ellington, 1984*c*,*d*). The creation of large persistent circulations has been verified for low Reynolds number flow by Maxworthy (1979). The circulation generated per unit length, Γ, may exceed the value that would be

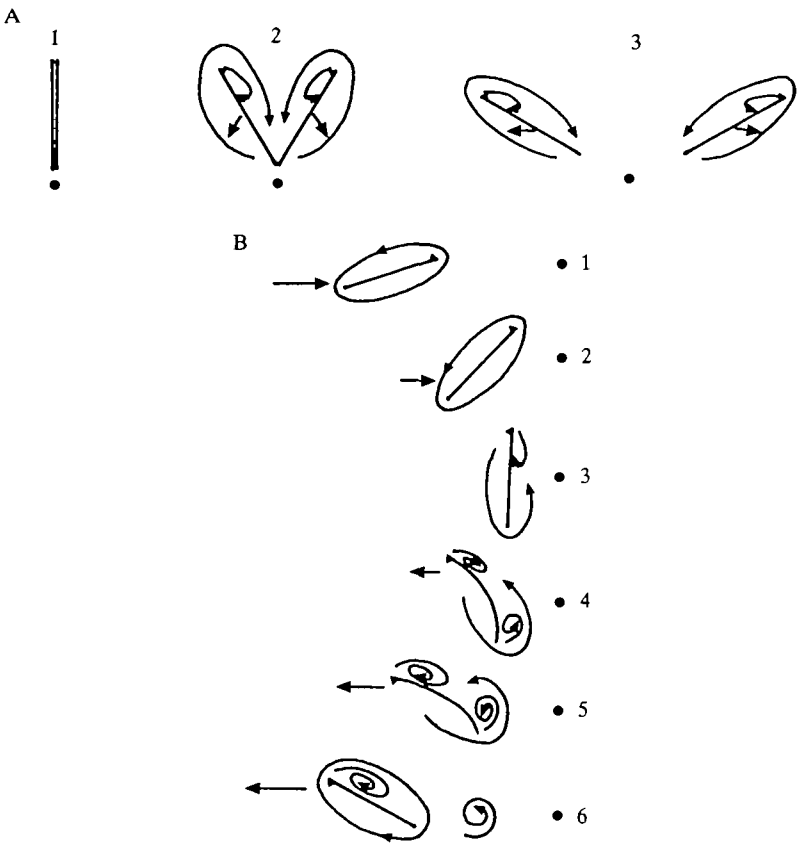

Fig. 1. Unsteady mechanisms of lift generation. (A) Clap-and-fling (after Weis-Fogh, 1973); top view of wing chord. (B) Flex (after Ellington, 1984*d*); side view of wing chord. In both diagrams, the wing chord is shown with a triangle on the upper leading edge. The solid circles represent a stationary reference point. Large-headed arrows represent motion of the wing: small-headed arrows, motion of the air. The mechanisms are explained in the text.

created by steady translation of the wing: it will depend on the rate, ω, at which the wings rotate and on the chord length, c, so that:

$$\Gamma = \gamma\omega c^2,$$

where the coefficient γ has a value of around 2, or even more for the peel. Clap-and-fling is used at the beginning of each downstroke by many small insects such as the chalcid wasp *Encarsia formosa* in which it was first described. It also seems to be used intermittently by larger insects when large values of lift are required, especially during take-off (Ellington, 1984*c*), and also by some birds and bats.

Unsteady mechanisms in isolated wings

The clap-and-fling mechanism cannot be the one used by hoverflies during

inclined stroke plane hovering because the wing beat amplitude is small and the wings do not approach each other. Weis-Fogh (1973) suggested that circulation was created at the leading edge by the isolated flexing of the wing along a longitudinal flexion line, a mechanism which he dubbed the 'flip'. As Ellington (1984*d*) noted, however, the wing would then have to unflex, creating opposite vorticity at the trailing edge and no net force would result.

Instead, Ellington suggested a mechanism relying on the gross vorticity changes produced by rotation, while the flexion of the wing merely controlled the pattern of vortex shedding. In this 'flex' mechanism (Fig. 1B) wing rotation at the end of the wing beat (2,3) increases the vorticity around the wing. Vorticity of the opposite sense must therefore be produced to satisfy Kelvin's circulation theorem. The trailing edge is almost stationary at this time because of the flexion of the wing, and this vorticity is therefore produced at the moving leading edge where shear stresses will be higher (3,4). This vorticity may finally reattach as the translation of the next stroke occurs (5,6), while the previous bound vortex rolls up at the trailing edge and is left behind (4,5,6). The trailing edge has to remain stationary during rotation, but flexion is not strictly necessary since this may also occur if mid rotation is delayed until just after stroke reversal, in effect allowing the wing to 'rotate around its trailing edge'.

In hoverflies hovering with an inclined stroke plane Ellington found that pronation was delayed until just after the start of the downstroke. During wing rotation the velocity of the leading edge was therefore high, whereas that of the trailing edge was zero. This would cause a large circulation to be built up which could attach to the wing. At the bottom of the stroke supination was advanced, resulting in greater movement of the trailing edge during rotation. The new circulation would therefore tend to build up around the trailing edge of the wing. It would be easily shed as the wing accelerated into the upstroke, during which little lift would be produced. The mechanism therefore gives potential for differential control of upstroke and downstroke circulation and hence the direction of the force produced by the wings, merely by altering the timing of wing rotation. Flex could be widely used by insects, and Ellington has calculated that it could create circulations as high as $1{\cdot}6\omega c^2$, or more in the case of delayed rotation, but it remains to be experimentally verified.

A further pattern of movement has been observed at the bottom of the downstroke in *Encarsia* (Weis-Fogh, 1973) and *Calliphora* (Wootton, 1981). Transverse flexion (as opposed to the longitudinal flexion seen in hoverflies) occurs near the wing base and the wing bends downwards without rotating. It then suddenly straightens, leading edge first, causing a fast rotation to a low upstroke angle of attack. It is possible that this could be a means of providing a strong 'flex' circulation for the upstroke, by delaying and speeding up supination. Nachtigall (1979) described three 'instationary' mechanisms which may operate in insect flight but he gave little explanation of the movement of vortices. Apart from the 'fast supination' mechanism which may describe the kinematics outlined above, they are unlikely to affect the force balance.

Symbols and abbreviations

A_o	Area of the actuator disc.
$\mathcal{A}R$	Aspect ratio of a pair of wings.
c	Chord of the wing.
$\bar{c}$	Mean chord.
C_D	Drag coefficient.
C_{Dpro}	Profile drag coefficient.
C_L	Lift coefficient.
D	Drag.
d/u	Ratio of duration of downstroke to upstroke.
$\hat{f}$	Non-dimensional impulse frequency.
g	Gravitational acceleration.
J	Body velocity/mean wing tip velocity.
J_R	Body velocity/mean velocity at $\hat{r}_1(v)$.
K	Maximum lift-to-drag ratio.
L	Lift.
$\hat{L}$	Mean lift divided by weight.
m	Mass of an insect.
m_v	Virtual mass of one wing.
m_w	Mass of one wing.
m_1, m_2	First and second moments of wing mass.
n	Wing beat frequency.
p_w	Wing loading.
P^*_{RF}	Rankine–Froude estimate of specific induced power.
r	Radial position along the wing.
$\hat{r}_k(m)$	Non-dimensional radius of the kth moment of wing mass.
$\hat{r}_k(s)$	Non-dimensional radius of the kth moment of wing area.
$\hat{r}_k(v)$	Non-dimensional radius of the kth moment of wing virtual mass.
R	Wing length.
Re	Reynolds number.
s_1, s_2, s_3	Moment of wing area.
S	Total wing area.
t	Time.
U	Wing velocity.
$\bar{U}_v$	Average flapping velocity.
v	Virtual mass of a wing.
V	Velocity of the body.
$\hat{V}$	Wing lengths travelled per wing beat.
$\bar{V}_f$	Average flapping velocity of a wing.
w_o	Induced velocity.
β	Stroke plane angle.
β_r	Relative stroke plane angle.
γ	Rotational lift coefficient.

Γ	Circulation.
η	Roll angle.
θ	Angle of elevation of wing relative to stroke plane.
ξ	Angle between mean flight path and horizontal.
ν	Kinematic viscosity of air.
ρ	Mass density of air.
τ	Temporal correction factor for induced velocity.
ϕ	Angle of wing along stroke plane.
Φ	Stroke angle.
χ	Angle between longitudinal body axis and horizontal.
ψ_A	Angle of aerodynamic force vector from vertical.
ψ_C	Calculated angle of aerodynamic force.
ω_p	Angular velocity during pronation.
ω_s	Angular velocity during supination.
$\hat{\omega}$	Angular velocity/wing beat frequency.

Materials and methods

Seven locally available species, representing some of the principal phylogenetic groups of Diptera and possessing contrasting flight behaviour, were filmed. These were the crane fly, *Tipula paludosa* Meigen, the March fly *Bibio marci* Linnaeus, the black fly *Simulium* Latreille, sp. indet. (Nematocera), the drone fly *Eristalis tenax* (Linnaeus), (Cyclorrhapha: Aschiza) (see Ellington, 1984*a–f*), *Conops strigatus* Weidemann in Meigen, the fruit fly *Drosophila melanogaster* Meigen, (Cyclorrhapha: Acalyptrata), and the bluebottle *Calliphora vicina* Robineau-desvoidy, (Cyclorrhapha: Calyptrata). Apart from being filmed, these insects were also subjected to a parallel study of thoracic morphology (Ennos, 1987), and of the structure and engineering of the wings (Ennos, 1988, 1989).

Filming

The insects were filmed in still air in relatively large flight boxes (Fig. 2). Insects

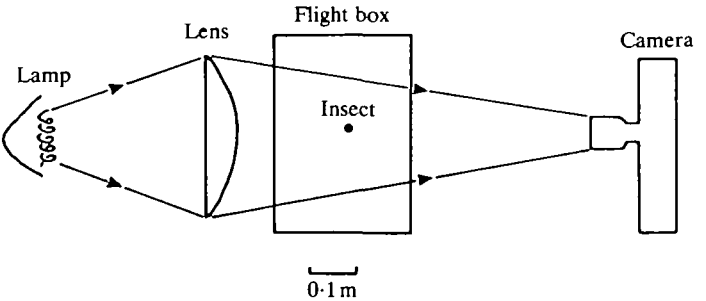

Fig. 2. The filming set-up. Insects were filmed in silhouette, illuminated from behind by light focused onto the film plane.

were back-illuminated using an 800 W 'redhead' ciné light (Rank Strand Ltd) which was focused onto the image plane of the Hyspeed ciné camera (John Hadland Photographic Instruments Ltd). This gave a less intense illumination than the method of Ellington (1984*c*). The insects were filmed at 3000–5000 frames s^{-1}, with a timing light marking the film every millisecond. A zoom lens fitted with close-up extensions of 1 or 2 dioptres provided focal distances ranging from 25 cm for *Drosophila* to 90 cm for the larger flies. The projected wing length of a filmed insect was approximately one-eighth to one-sixth of the frame length to allow the flight pattern of insects to be ascertained. Apertures varied from f8 to f16. Pan F or FP4 film was used and the negatives were developed and used for subsequent analysis.

Most insects were filmed in a Perspex flight cage 45 cm high and 30 cm square. *Simulium* and *Drosophila* were filmed in smaller cages, 20 cm high and 10 cm square and 8 cm in diameter by 5 cm deep, respectively.

Various techniques were used to obtain film. *Eristalis* males hovered freely in a well-lit flight chamber in which their favourite composite flowers had been placed, patrolling the sides of the cage as if it was their territory. Film was obtained by using a crossed-beam detector system designed by Newman (1982) which triggered the camera when the insect was in the field of view. The same set-up was fortuitously successful in obtaining a film of *Conops*.

Bibio was filmed when taking off from a Perspex tube positioned in the film frame. *Tipula* was filmed taking off from inside a 10 cm diameter polyethylene beaker. The film was triggered by hand.

The other insects were frequent fliers but tended to hover only rarely. Attempts to film individuals were quickly abandoned. Instead a 'cast of thousands' approach was adopted. Large numbers of insects, typically 50–100 were placed in the flight cage. It was then tapped to initiate flight in as many individuals as possible and the camera was manually triggered. At any one time only one or two flies were generally observed to be flying in the film frame, and they were always separated by several wing lengths. There would consequently be little interference between flies and the air could be regarded as being 'still'. This approach to filming prevents exact analyses of forces being achieved since the exact morphology of individuals is unknown, but average values could be calculated and used to give good estimates. A great deal of information could, therefore, be quickly amassed.

Morphology of insects

After filming an individual, some of the morphological measurements described and explained by Ellington (1984*b*) were made, for use in aerodynamic calculations.

First, the insect was weighed to find its mass, m, to the nearest one-tenth of a milligram. It was then killed with ethyl acetate vapour and the left wing was removed, cutting as close to the wing base as possible, and weighed, yielding the wing mass, m_w. The wing was then cut into 2 mm strips from the base, parallel to the wing chord, with a razor blade and each strip was weighed. From these

measurements the first and second moments of wing mass, m_1 and m_2, around the base could be calculated using the formula:

$$m_k = \sum m_i r^k, \tag{1}$$

for k equalling 1 and 2, respectively, where m_i is the mass of a wing strip and r is the perpendicular distance of the midline of the strip from the wing base. The non-dimensional radii, $\hat{r}_1(m)$ and $\hat{r}_2(m)$ were then calculated using the formula:

$$\hat{r}_k{}^k(m) = m_k / \sum m_i R^k, \tag{2}$$

where R is the wing length.

The right wing was then removed and placed between a microscope slide and cover slip. This was placed in a photographic enlarger and an image produced at a magnification of 10×. This image was traced onto graph paper and the length of the wing R found. The total wing area, S, was found by measuring the area of the cut out image with a leaf area meter manufactured by Delta T Devices Ltd, Cambridge, England. From these values the wing aspect ratio $\mathcal{A}R$ could also be calculated using the formula:

$$\mathcal{A}R = 4R^2/S \tag{3}$$

and the wing loading p_w:

$$p_w = mg/S. \tag{4}$$

The wing image was then cut into 1 cm strips (representing 1 mm wing strips) parallel to the wing chord and the area of each of the strips was found with the area meter. From these measurements the first to third moments of wing area s_1 to s_3 were calculated, using the formula:

$$s_k = 2\sum s_i r^k \tag{5}$$

for values of k from 1 to 3, where s_i is the area of each strip and r is the distance of its midline from the wing base. The non-dimensional radii of area could then be found from:

$$\hat{r}_k{}^k(s) = s_k / SR^k. \tag{6}$$

The moments of virtual mass, the mass of air which is bound to an accelerating wing, and is approximately equal to the mass of the cylinder of air of diameter equal to the local wing chord, c, can also be found. For the purposes of the calculation, the chord of each wing strip was regarded as being equal to its area divided by its width, 1 mm. The virtual mass of each wing strip, v_i; is therefore given by the formula:

$$v_i = \pi\rho(s_i/1000)^2/4, \tag{7}$$

where ρ is the density of air. The total virtual mass m_v is the sum of all the values of v_i.

The moments of virtual mass and the values for the first and second radii of

Table 1. *Gross morphological parameters*

Insect	Sex	m (mg)	R (mm)	S (mm^2)	p_w ($N\,m^{-2}$)	m_w (mg)	m_v (mg)
Tipula paludosa							
Tp.1	M	45·4	17·0	110·4	4·0	0·557	0·194
Tp.2	M	39·5	15·8	87·2	4·4	0·441	0·130
Tp.3	M	49·6	16·8	97·2	5·0	0·471	0·151
Bibio marci							
Bm.1	F	65·4	11·2	75·2	8·5	0·224	0·134
Bm.2	M	26·6	9·4	49·0	5·3	0·149	0·070
Bm.3	M	31·0	9·4	48·6	6·3	0·165	0·068
Conops strigata							
Cs.1	M	27·1	7·7	30·0	8·8	0·076	0·031
Eristalis tenax							
Et.1	M	97·9	11·5	72·4	13·2	0·370	0·117
Et.2	M	103·6	11·2	70·6	14·4	0·365	0·112
Et.3	M	95·0	10·8	68·0	13·7	0·340	0·110
Calliphora vicina							
Cv.		62·0 ±4·7	9·2 ±0·5	57·8 ±2·0	10·7 ±0·8	0·235 ±0·009	0·091 ±0·004
Simulium							
Sm.		0·80 ±0·29	3·26	8·2	0·98	NA	0·0049
Drosophila melanogaster							
Dm.		0·72 ±0·12	2·02	2·6	2·77	NA	0·0008

The mass, m, the wing length, R, the wing area, S, the wing loading, p_w, the wing mass, m_w, and the wing virtual mass, m_v, for insects of each species.
NA = not available.

virtual mass $\hat{r}_1(v)$ and $\hat{r}_2(v)$ can then be calculated in just the same way as the moments of mass, substituting values of v_i for values of m_i in equations 1 and 2.

The non-dimensional virtual mass is given by:

$$\hat{v} = v\mathcal{A}R^2/2\pi\rho R^3, \tag{8}$$

which is the ratio of virtual mass to that of a wing with a constant chord width equal to the average value of the chord.

Gross morphological measurements are given in Table 1 and shape parameters in Table 2. For insects which were filmed by the cast of thousands method, average values of the mass and wing length of 10 animals were found. For *Calliphora* the wings of four animals were measured to give values for other wing parameters. The wings of *Drosophila* and *Simulium* were too small for analysis of mass parameters, and shape parameters were subject to large error. Shape parameters of one insect of each species are therefore given.

Table 2. *Shape parameters of the study insects*

Insect	$\mathcal{AR}$	$\hat{r}_1(s)$	$\hat{r}_2(s)$	$\hat{r}_3(s)$	$\hat{v}$	$\hat{r}_1(v)$	$\hat{r}_2(v)$	$\hat{r}_1(m)$	$\hat{r}_2(m)$
Tipula paludosa									
Tp.1	10·42	0·549	0·598	0·635	1·15	0·566	0·602	0·43	0·50
Tp.2	11·47	0·547	0·595	0·631	1·16	0·565	0·600	0·47	0·54
Tp.3	11·61	0·549	0·599	0·636	1·14	0·569	0·605	0·45	0·52
Bibio marci									
Bm.1	6·67	0·498	0·552	0·594	1·14	0·488	0·531	0·38	0·45
Bm.2	7·21	0·488	0·541	0·582	1·13	0·474	0·515	0·38	0·45
Bm.3	7·19	0·504	0·557	0·598	1·16	0·488	0·531	0·38	0·46
Conops strigata									
Cs.1	7·89	0·540	0·593	0·630	1·11	0·561	0·598	0·33	0·40
Eristalis tenax									
Et.1	7·30	0·472	0·534	0·579	1·09	0·462	0·512	0·33	0·42
Et.2	7·12	0·475	0·538	0·584	1·07	0·462	0·514	0·33	0·41
Et.3	6·87	0·478	0·539	0·584	1·08	0·467	0·514	0·32	0·41
Calliphora vicina									
Cv.	5·90	0·477	0·540	0·587	1·08	0·464	0·516	0·31	0·38
	±0·10	±0·002	±0·003	±0·003	±0·01	±0·002	±0·003	±0·01	±0·01
Simulium									
Sm.	5·32	0·453	0·519	0·567	1·07	0·428	0·485	NA	NA
Drosophila melanogaster									
Dm.	6·37	0·490	0·545	0·586	1·08	0·495	0·536	NA	NA

The aspect ratio, $\mathcal{AR}$, and the non-dimensional radii of area, (s), mass (m), and virtual mass, (v), and the non-dimensional virtual mass, $\hat{v}$, for insects of each species.

Film analysis

Each wing beat was analysed by the method of Ellington (1984*c*), using the translation into BBC BASIC of his analysis program by Robert Dudley. The analysis relies on three conditions: the wing beat must be symmetrical; one wing, with its base visible, must cross the image plane during the beat, so giving the maximum projected wing length; and the wings must not bend appreciably. For this reason some interesting turns could not be quantitatively analysed.

For film analysis the ciné negative image was back-projected onto a frosted glass viewing screen to give a frame size of approximately 45 cm × 30 cm. The image was digitized using a photo-optical data analyser manufactured by L. W. International, Woodland Hills, California. This had a resolution of 0·1 mm, approximately 0·2 % of projected wing length and certainly better than the accuracy with which individual points on the frame could be identified.

In some of the insects the wings bent ventrally by up to 40°. This occurred only about 10–15 % of the wing length from the base, however, and so the projected wing length was reduced by at most 2 %. It was assumed that the resulting errors of

wing position were at most 2–3° since when the wings were most flexed they were well away from the image plane.

For each frame of an analysed wing beat, including a few frames overlapping the start and finish of the stroke, six points were digitized: a reference mark, one wing base, both wing tips and the front and rear tips of the body. The program then calculated the following parameters.

(a) *Body parameters.* (i) The roll angle, η, of the insect. (ii) The angle of the body axis to the horizontal, χ (positive when the head is above the body).

(b) *Wing parameters.* (i) The stroke plane angle, β, of the wing relative to the horizontal (positive when the wing moves downwards on the morphological downstroke). This is calculated by linear regression of all the frames. (ii) The instantaneous position of the wing along the stroke plane, ϕ, positive when the wing is raised towards the top of the stroke. (iii) The instantaneous elevation of the wing, θ, positive when the wings are above the stroke plane through the wing base. From the maximum, ϕ_{max}, and minimum, ϕ_{min}, values of wing position the stroke amplitude, Φ, can be found. Some of these parameters are illustrated in Fig. 3A.

(c) *Flight parameters.* (i) Non-dimensional flight velocity, $\hat{V}$, measuring the speed of the insect in wing lengths per wing beat. The advance ratio, J, defined by Ellington (1984*c*), is the ratio of flight velocity to the mean wing tip velocity, and is given by the equation $J = \hat{V}/2\Phi$. (ii) The flight trajectory of the insect, ξ, positive for upward flight.

The results are given in Table 3. The errors inherent in such an analysis are discussed by Ellington (1984*c*).

The frequency of the wing beat was calculated using the light markers on the film. The time for a wing beat was measured between the middle of successive pronations, estimated visually on the film. It was assumed for the purposes of the analysis that the film was running through the camera at a constant speed. This assumption produced at worst a 2% error in the timing of any one frame.

The angle of attack of the wing was visually estimated throughout the wing beat. During pronation and supination the average angular velocity of the wing $\hat{\omega}_p$ and $\hat{\omega}_s$ (in radians per wing beat) was calculated after the method of Ellington (1984*c*). A further dimensionless number, $\hat{\omega}/\Phi\mathcal{A}R$, was also calculated for each case. This compares the velocity of the wing edges at stroke reversal due to this angular velocity with that of the mean wing tip velocity during wing translation. The results are given in Table 4, but it must be remembered that because of the large error inherent in their calculation both these sets of values should only be taken as order of magnitude estimates.

Results

The film sequences

The film sequences were chosen to show as wide a range of flight behaviour as possible. In the small flight cages it would be impossible for insects to achieve high speeds and so fast forward flight is under-represented. It is difficult to calculate the

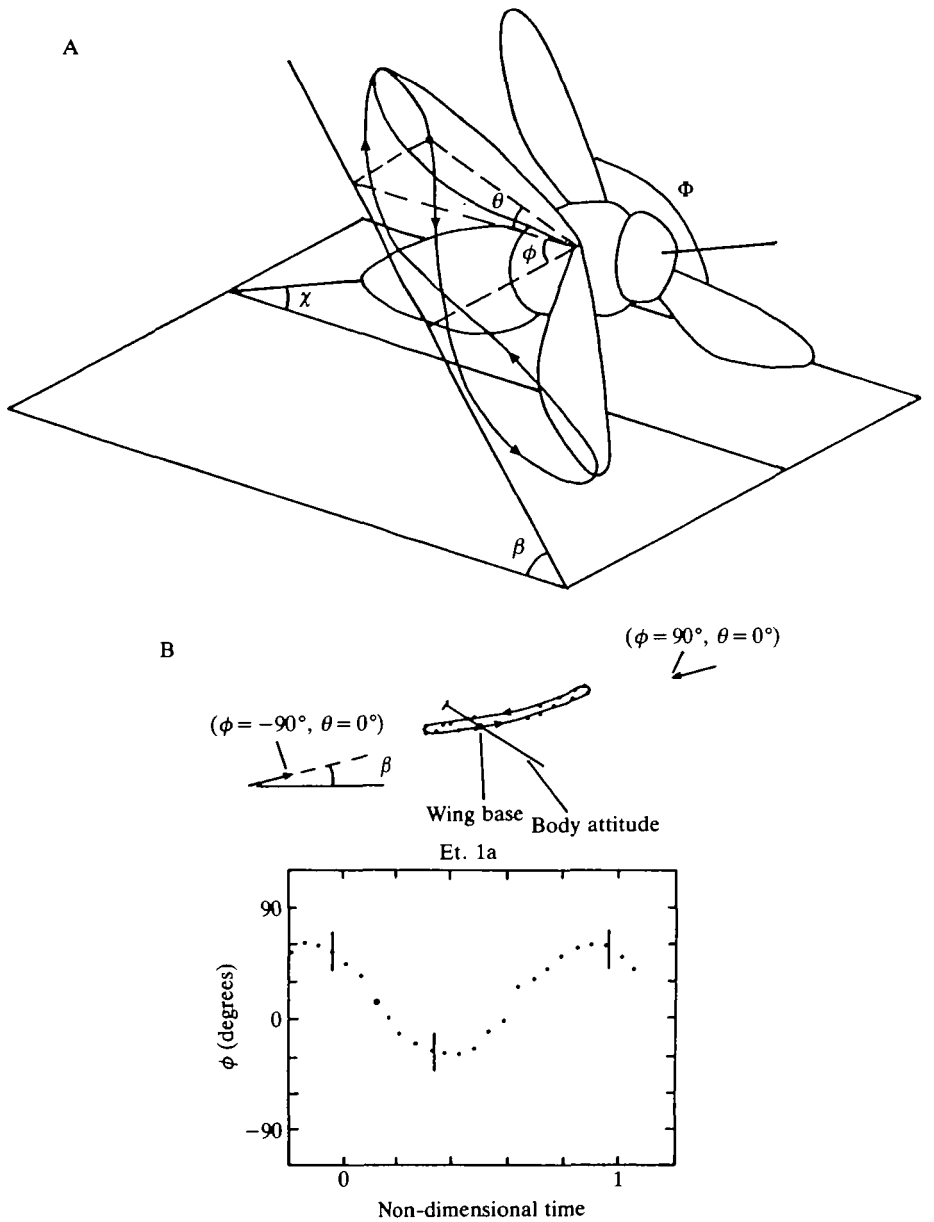

Fig. 3. The kinematics of flight. (A) Kinematic parameters measured for each sequence: body angle, χ; stroke plane angle, β; stroke amplitude, Φ; and instantaneous positions of the wing along the stroke plane, ϕ; and above the stroke plane, θ. (B) Results for the hoverfly *Eristalis tenax* (Et.1a). Wing motion in time and space is shown as explained in the text, together with the body attitude and velocity.

Table 3. *Kinematics of flight sequences*

Sequence	β (degrees)	$\bar{\chi}$ (degrees)	η (degrees)	ϕ_{max} (degrees)	ϕ_{min} (degrees)	Φ (degrees)	n (Hz)	d/u	$\bar{V}$	ξ (degrees)	J
Et.1a	14·1	32	8	59	−27	86	183	0·85	0	0	0
Et.1b	14·9	30	3	59	−41	100	172	0·92	0	0	0
Et.1c	12·0	33	1	60	−36	96	169	0·89	0	0	0
Et.3a	13·7	16	4	58	−40	98	172	0·90	0	0	0
Et.3b	12·1	19	24	65	−42	107	173	0·99	0·40	9	0·11
Bm.1a	34·0	13	4	95	−44	139	99	1·09	0	0	0
Bm.1b	10·2	28	9	91	−51	140	101	1·17	0·67	32	0·14
Bm.2	5·9	37	23	79	−59	138	130	1·06	0·78	57	0·17
Cv.1	−12·6	82	17	83	−67	150	117	0·87	0	0	0
Cv.2	−16·5	63	7	81	−53	134	152	0·89	0·68	46	0·15
Cv.3	20·0	39	15	74	−49	123	138	1·03	0·31	61	0·07
Cv.4	47·1	6	22	85	−61	146	158	1·12	1·60	−10	0·32
Dm.1	−10·9	60	1	73	−63	136	254	0·83	0·75	63	0·16
Dm.2	28·5	32	31	91	−71	162	229	0·98	1·80	15	0·33
Sm.1	14·0	49	20	85	−64	149	183	1·36	2·51	11	0·50
Cs.1	7·2	24	17	82	−62	144	144	1·36	0·39	35	0·11
Tp.3	31·2	19	2	87	−25	112	59	0·96	0·50	39	0·13

The stroke plane angle, β, the body angle, $\bar{\chi}$, the roll angle, η, the angle of the wing along the stroke plane at the top, ϕ_{max}, and bottom, ϕ_{min}, of the beat, and the stroke amplitude, Φ, the wing beat frequency, n, the ratio of the downstroke to upstroke duration, d/u; the non-dimensional flight velocity, $\bar{V}$, the flight angle, ξ, and the advance ratio, J, for each flight sequence.

direction of the aerodynamic force in insects which are turning or accelerating and so, in general, only sequences of steady flight were digitized, though films of turns and other manoeuvres were studied qualitatively.

Eristalis tenax males hovered well in the flight cage and four hovering sequences are shown. To demonstrate the kinematics of an animal hovering apparently steadily, three sequences were taken of the same individual, Et.1, at intervals of approximately 0·1 s. Although the stroke plane angle remains inclined at around 13° ($\Delta\beta = 2{\cdot}9°$), the stroke amplitude is very variable ($\Delta\Phi = 14°$). The hoverfly Et.3 first hovered and then turned and accelerated out of the film frame, without changing its stroke plane angle significantly ($\Delta\beta = -1{\cdot}6°$).

Two good films were obtained of the take-off and rising flight of *Bibio marci*. The two sequences of Bm.1, a female, are particularly interesting. After take-off it first hovered with a stroke plane inclined by around 30° with the wings performing a clap-and-fling at the top of the stroke (Bm.1a). It then accelerated upwards and forwards, while reducing the stroke plane angle and the wing beat amplitude (Bm.1b). The kinematics of hovering can thus be compared with those of forward rising flight. The rising flight of a lighter male March fly (Bm.2) is analysed for comparison.

Table 4. *Rotational velocities of pronation and supination*

	Pronation		Supination	
Sequence	$\hat{\omega}$	$\hat{\omega}/\Phi\mathcal{A}R$	$\hat{\omega}$	$\hat{\omega}/\Phi\mathcal{A}R$
Et.1a	8·0	0·72	8·0	0·72
Et.1b	10·0	0·79	10·1	0·79
Et.1c	9·0	0·73	7·1	0·58
Et.3a	9·3	0·79	8·0	0·69
Et.3b	7·4	0·58	7·4	0·58
Bm.1a	10·5	0·64	8·5	0·52
Bm.1b	14·6	0·86	10·9	0·64
Bm.2	18·0	0·94	7·5	0·40
Cv.1	11·8	0·75	11·7	0·74
Cv.2	8·5	0·61	14·3	1·02
Cv.3	12·8	0·99	12·7	0·99
Cv.4	10·5	0·69	12·7	0·83
Dm.1	8·6	0·57	8·6	0·57
Dm.2	12·5	0·69	13·7	0·76
Sm.1	10·4	0·75	13·3	0·96
Cs.1	16·0	0·80	18·7	0·94
Tp.3	9·6	0·43	11·6	0·51

The approximate values of non-dimensional rotational velocity, $\hat{\omega}$, in radians per wing beat at both pronation and supination for each sequence.

The ratio of rotational to the average flapping velocity of the wing edge, $\hat{\omega}/\Phi\mathcal{A}R$, is also given.

For *Calliphora vicina*, one hovering sequence (Cv.1) was obtained, along with two sequences of forward rising flight (Cv.2,3) and one of fast forward flight (Cv.4). *Calliphora* seemed to hover with a *negatively* inclined stroke plane and a near vertical body. The stroke plane during rising flight was very variable, but could also be negatively inclined. These unusual kinematics are investigated.

Drosophila melanogaster seemed to have a similar flight pattern to *Calliphora* and two sequences show it in forward rising flight with a negatively inclined stroke plane (Dm.1) and in fast forward flight (Dm.2).

It proved more difficult to obtain film of the other insects and there is only a single flight sequence for each. *Tipula paludosa* (Tp.3) is filmed accelerating into forward flight, *Conops strigatus* (Cs.1) is captured in slow forward flight, and *Simulium* (Sm.1) is in fast forward flight with a rather shallow stroke plane angle.

Quantitative results

The results of digitization are given in Table 3 and the kinematics are also drawn in Figs 3–7, which are similar to those of Ellington (1984*c*). In each case, the upper figure shows the inclination of the body, pointing to the left and upwards, and the wing base, represented by a large solid circle. The wing tip path is shown as a plot of θ, the instantaneous position above the stroke plane, against ϕ, the instan-

taneous position along the stroke plane. The scale is set by the arrows whose tips point at values of ϕ of 90° and −90° and values of θ of 0. The non-dimensional flight velocity $\hat{V}$ is shown as an arrow leaving the wing base. It is drawn to scale when it is greater than 0·1, a flight velocity of 1 wing length per wing beat having a length equal to the distance from the wing base to the arrows giving the stroke

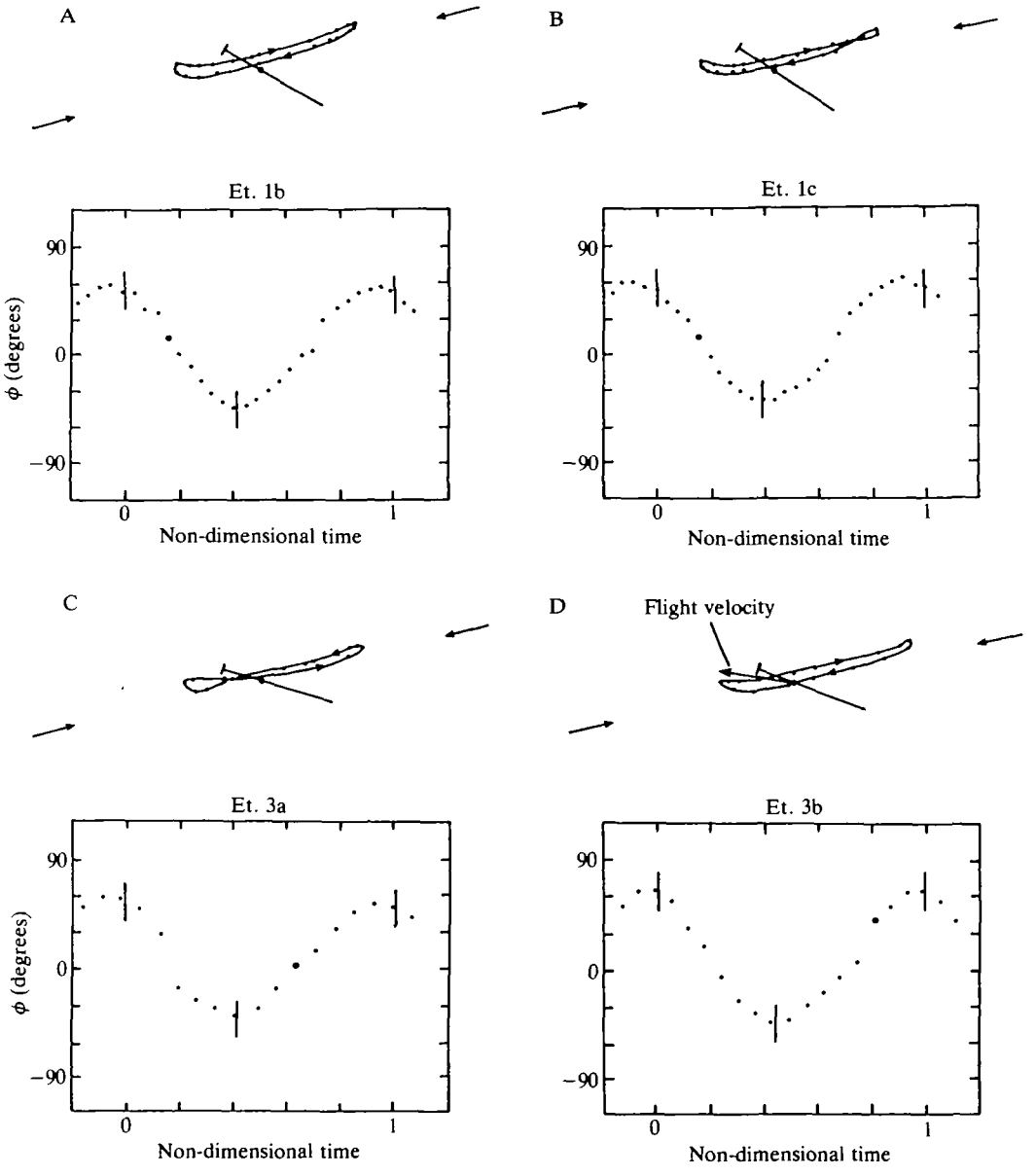

Fig. 4. Kinematics of (A) *Eristalis tenax* Et.1b; (B) *E. tenax* Et.1c; (C) *E. tenax* Et.3a; (D) *E. tenax* Et.3b. See text for explanation.

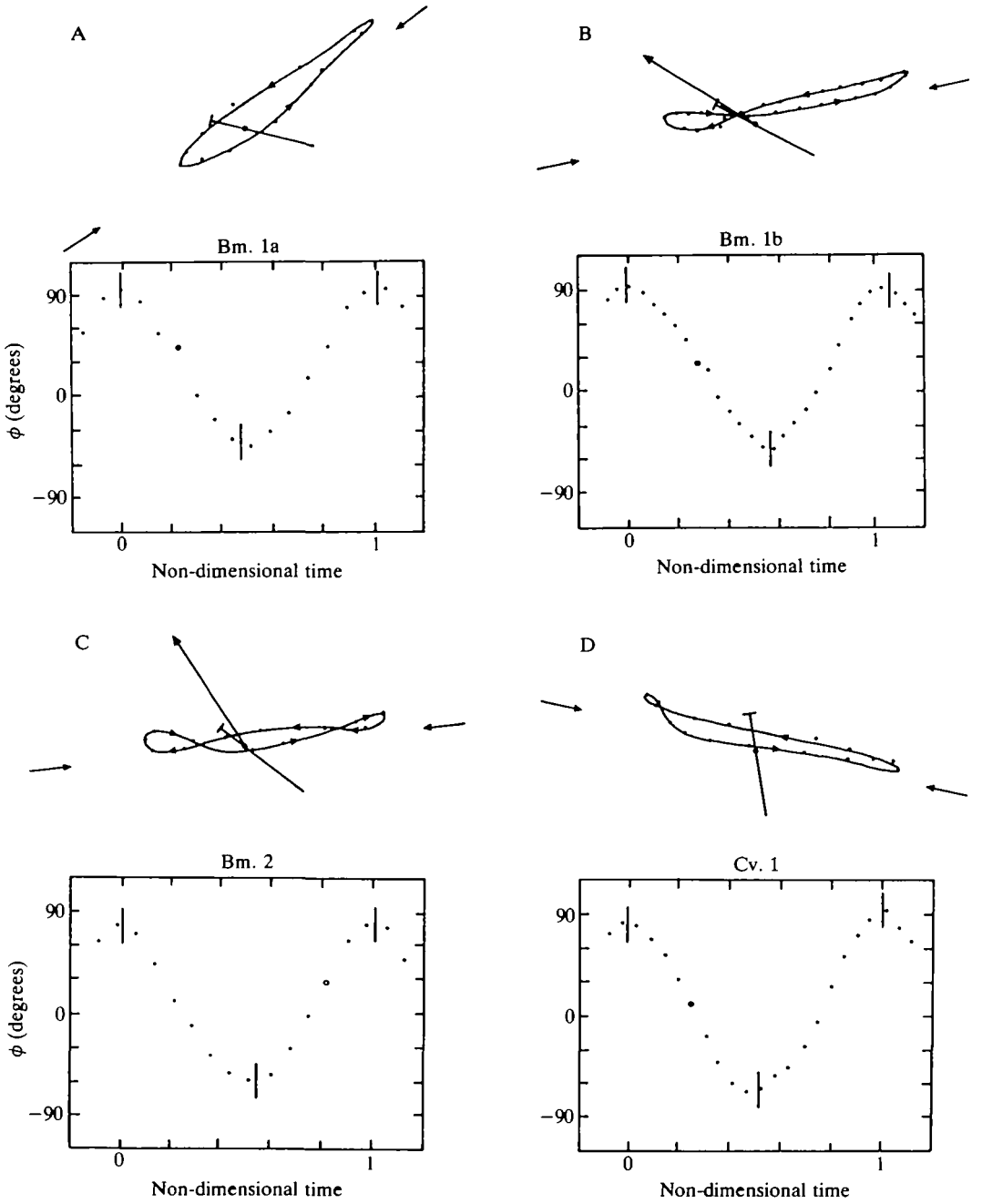

Fig. 5. Kinematics of (A) *Bibio marci* Bm.1a; (B) *B. marci* Bm.1b; (C) *B. marci* Bm.2; (D) *Calliphora vicina* Cv.1.

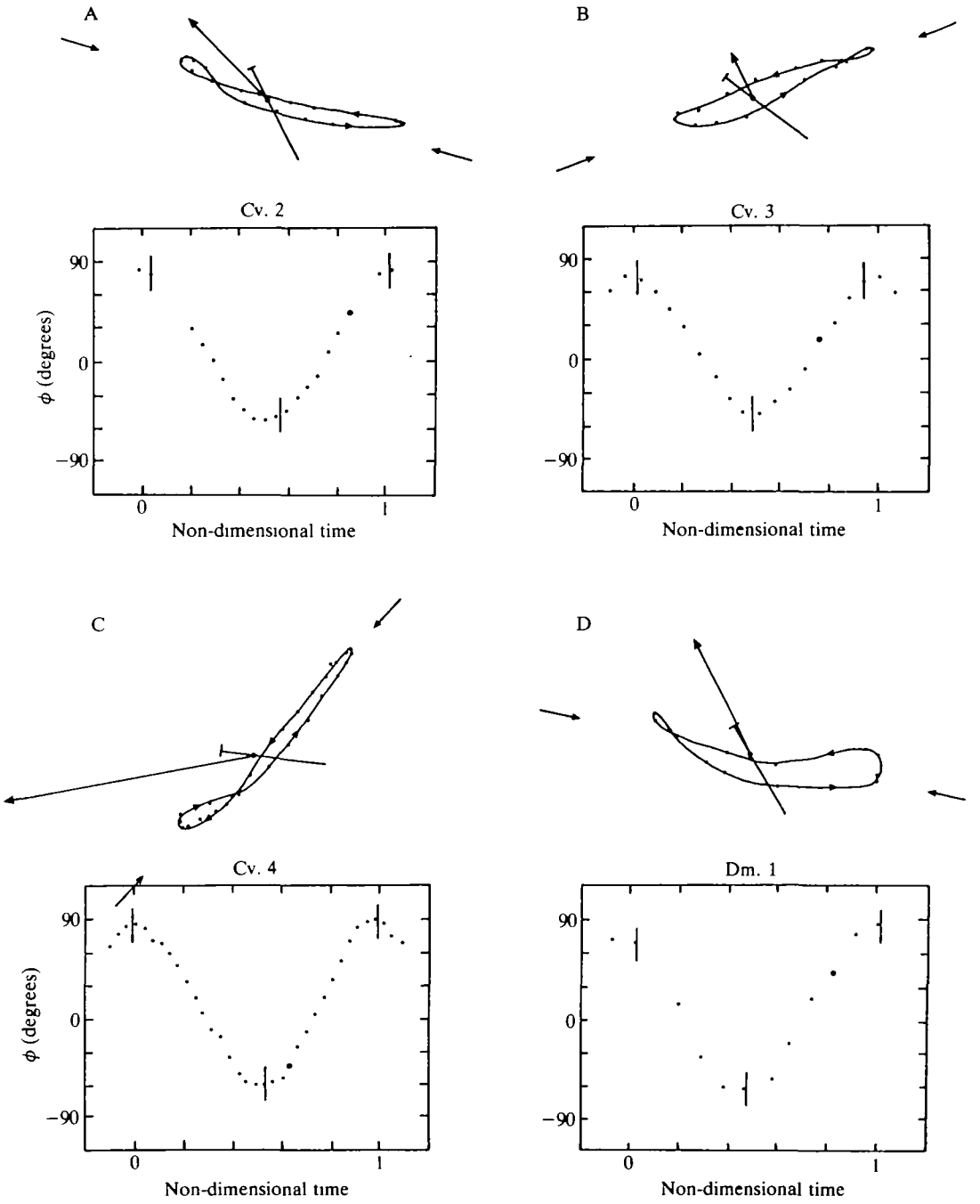

Fig. 6. Kinematics of (A) *Calliphora vicina* Cv.2; (B) *C. vicina* Cv.3; (C) *C. vicina* Cv.4; (D) *Drosophila melanogaster* Dm.1.

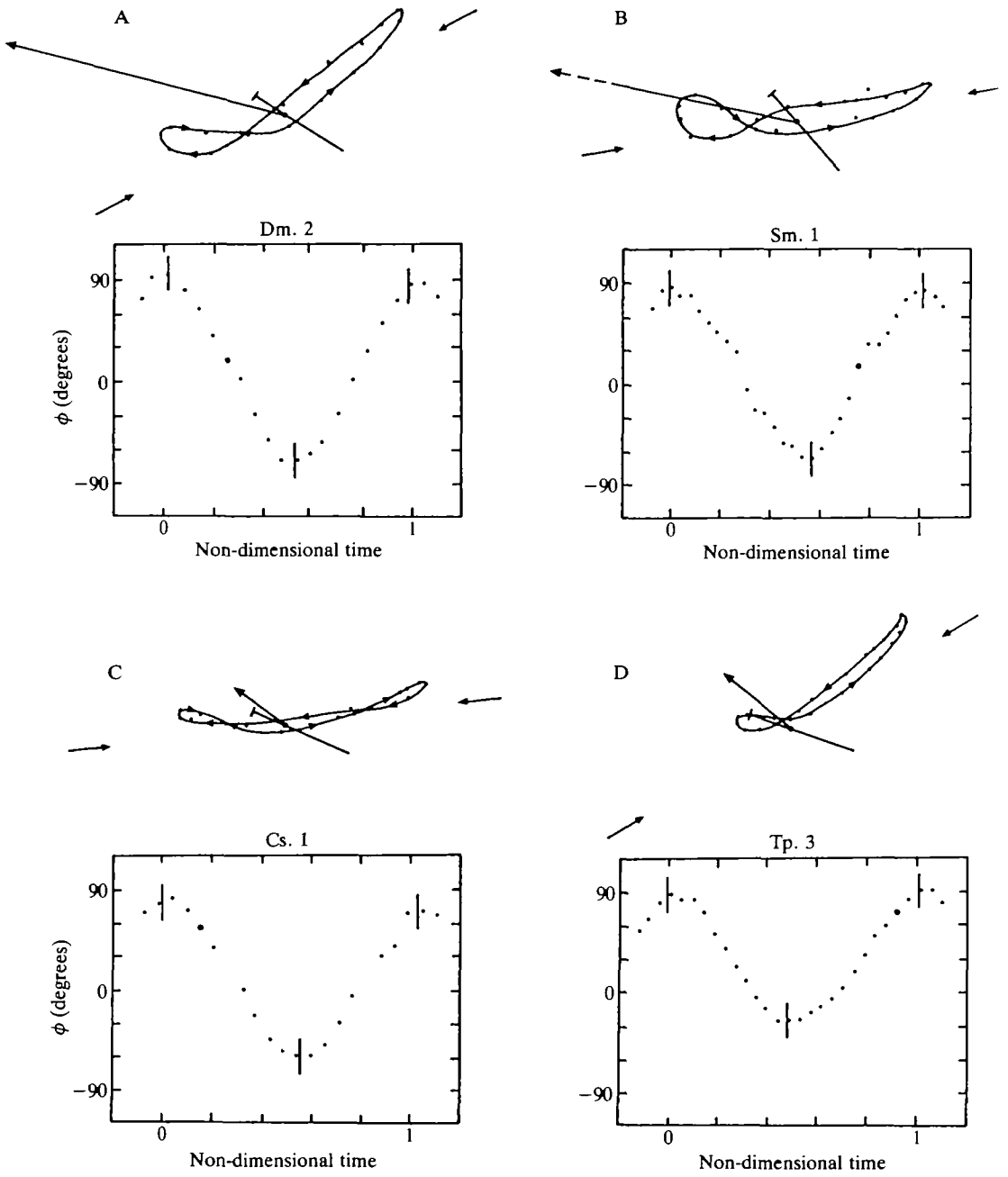

Fig. 7. Kinematics of (A) *Drosophila melanogaster* Dm.2; (B) *Simulium* Sm.1; (C) *Conops strigatus* Cs.1; (D) *Tipula paludosa* Tp.3.

plane. In the lower diagram the positional angle of the wing, ϕ, is drawn as a function of non-dimensional time. The middle of pronation and supination are represented by vertical bars on the graph. The frame in which the near wing has its

maximum projected length is subject to large errors and is shown in the lower figure as an open circle. It is not shown in the upper figure.

The non-dimensional rotational velocities $\hat{\omega}$ for pronation and supination are given for each sequence in Table 4 along with the relative velocities of rotation to translation, $\hat{\omega}/\Phi\mathcal{R}$.

Qualitative description of the wing beat

In all cases the wing beats of the flies were qualitatively similar to those found by Ellington (1984*c*). The wing tip moved back and forth along the stroke plane, its velocity differing little from simple harmonic motion, and generally rose above the stroke plane towards the end of each half-stroke. Individual differences will be discussed during the aerodynamic analyses of the sequences.

The attitude of the wing was changing throughout the beat. The wing pitch angle during both the downstroke and upstroke was positive, with the leading edge raised by approximately 30–45° at 0·7R. The values tended to be higher on the upstroke, as Nachtigall (1981) found in the rising flight of *Tipula*. During each stroke, however, the pitch did not appear to be 'set' as is generally reported. Instead, it rose gradually throughout the beat, especially during the upstroke. The speed of rotation gradually increased towards the end of the stroke when the wing was decelerating and reached a maximum approximately at stroke reversal. The wing then rotated further to an angle of attack some 10° below that adopted during the start of the next stroke and then recoiled. The process seems to be the result largely of inertial and aerodynamic forces acting on a compliant wing base but there is evidently some degree of control, for as in Ellington's sequences of the hoverfly *Episyrphus*, the timing of the middle of pronation and supination in *Eristalis* and in *Calliphora* was variable.

In all cases the wings deformed during the beat. During each half-stroke, the wing was twisted along its length so that the angle of attack was reduced towards the wing tip, a pattern that has been observed in flies by many previous authors (Nachtigall, 1966, 1981; Wootton, 1981; Ellington, 1984*c*; Dudley, 1987). The actual angles of torsion were small, around 10° for most species, though the wings of *Tipula* and *Simulium* twisted rather more and *Drosophila* wings rather less than average.

During each stroke, the wings also developed a positive camber which would increase their efficiency as aerofoils (Vogel, 1967; Dudley, 1987). The magnitude was generally small, a matter of a few percent of the wing chord, and the wings appeared to camber in a gentle curve, not localized to flexion lines. Camber was most obvious in *Eristalis*, *Bibio* and *Conops*, which possess stiff wings.

Both torsion and camber are reversed during stroke reversal when the wings rotate. The anterior distal part of the wing rotates first at stroke reversal, and this causes a camber of the correct sign for the coming half-stroke to be set up. As the rear and basal part of the wing subsequently rotates a 'tip to base torsion wave' runs through the wing (Wootton, 1981; Ellington, 1984*c*,*d*; Ennos, 1988) and much of this camber is lost.

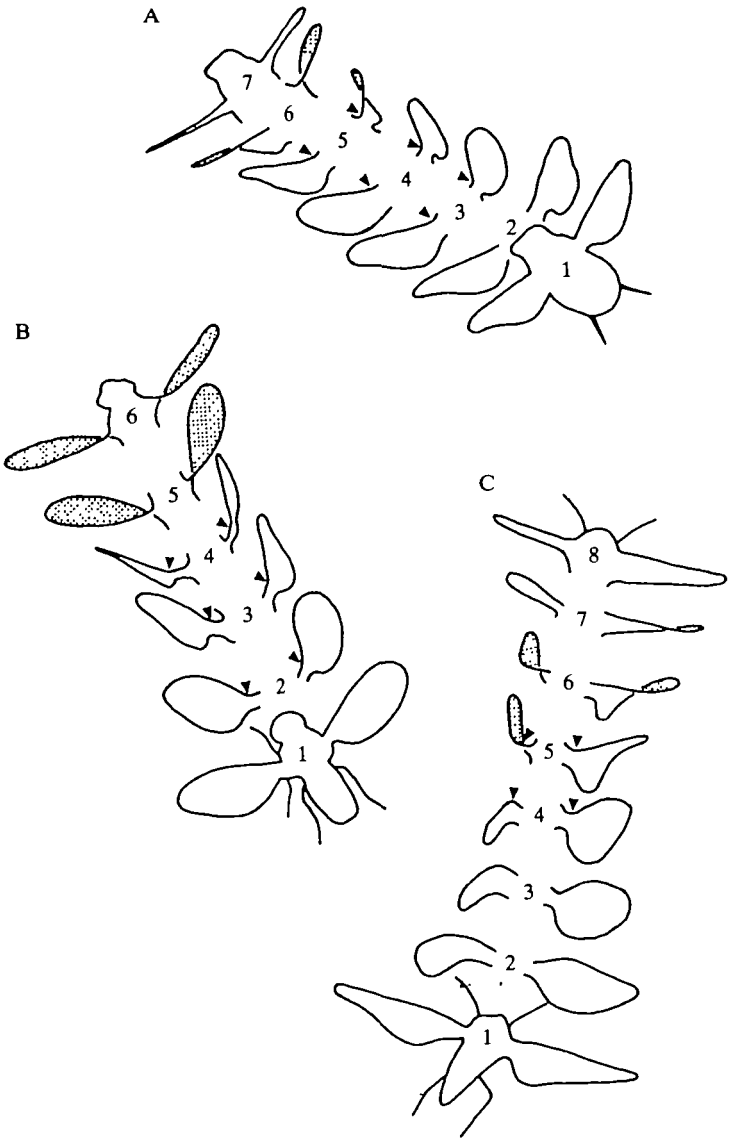

Fig. 8. Ventral wing flexion at the bottom of the downstroke. Film tracings of (A) *Calliphora*, (B) *Drosophila* and (C) *Simulium*. Oblique dorsal view of insects, with the ventral surface of the wings shown stippled. The position of flexion is shown by the arrowheads. The interval between frames is 0·2 ms.

Wings did not always remain straight. In insects of the three species that possess ventral flexion mechanisms, *Calliphora, Drosophila* and *Simulium*, the wing started to bend downwards from near the base towards the end of the downstroke when the wing was starting to decelerate (Fig. 8). At this point, the positional angle of the wing, ϕ, was approximately zero. The angle through which the wing

bent, therefore, tended to be greater when the downstroke limit, ϕ_{min}, was more negative. At the start of the upstroke, the leading edge of the wing suddenly straightened, causing a fast supination (Wootton, 1981). The wing, however, usually remained slightly bent ventrally until the top of the upstroke and did not show any camber.

Aerodynamic analysis of selected sequences

Hovering

Calculation of quasi-steady lift coefficients

The equations of Ellington (1984*e*,*f*) are used with suitable simplifications to estimate the lift and drag coefficients during each half-stroke and hence the relative weight support of the two strokes.

To calculate the relative velocity of the wings during each beat the induced velocity must first be found. According to the Rankine–Froude theory of propellers, the induced velocity is vertical and the momentum flux of the far wake must equal the weight of the insect. For periodic flapping, the mean induced velocity w_o at the wing plane was corrected by Ellington in his vortex theory, so that:

$$w_o = P^*_{RF}(1 + \tau) , \tag{9}$$

where P^*_{RF} is the Rankine–Froude estimate of specific induced power, and τ is the temporal correction factor due to the periodic nature of the force impulse.

$$P^*_{RF} = (mg/2\rho A_o)^{0.5} , \tag{10}$$

where A_o is the area $\Phi R^2 \cos\beta$ over which the wing imparts downward momentum so:

$$P^*_{RF} = (mg/2\rho\Phi R^2\cos\beta)^{0.5} . \tag{11}$$

The relative stroke plane angle can be found by vector addition of the mean induced velocity and the mean flapping velocity. This is taken as being the mean wing tip velocity, $2\Phi nR$.

$$\tan\beta_r = \tan\beta \pm P^*_{RF}(1+\tau)/2\Phi nR\cos\beta , \tag{12}$$

with a negative sign for the downstroke and a positive sign for the upstroke.

The correction factor, τ, is given by:

$$\tau = \frac{0{\cdot}632\pi p_w}{\rho \hat{f}^2 n^2 \Phi^2 R^2 A R \cos^2\beta} , \tag{13}$$

where p_w is the wing loading and $\hat{f}$ is the non-dimensional frequency, which equals 2 if both half-strokes provide weight support and 1 if only one does so. The values of τ are given in Table 5, both for equal weight support and for support by one stroke. The resultant stroke plane angles are given for both cases.

The lift coefficients can then be calculated using a simplified version of

Table 5. *Relative stroke planes and lift coefficients for hovering sequences*

	Relative stroke plane angle						Life coefficients			
	Equal support			One-stroke support			Quasi-steady		Rotational mechanisms	
Sequence	τ	β_{rD}	β_{rU}	τ	β_{rD}	β_{rU}	C_{LD}	C_{LU}	γ_D	γ_U
Eristalis tenax										
Et.1a	0·08	−1·0	27·0	0·30	−3·4	26·1	2·61	1·19	1·02	0·44
Et.1b	0·06	3·0	25·7	0·25	0·8	25·1	2·21	0·78	0·87	0·28
Et.1c	0·07	−0·8	23·7	0·29	−3·4	23·0	2·33	1·14	0·94	0·42
Et.3a	0·09	−0·5	26·4	0·35	−3·9	25·4	2·59	1·24	0·99	0·44
Bibio marci										
Bm.1a	0·11	22·6	43·0	0·43	18·8	42·2	4·42	0	1·55	0
Calliphora vicina										
Cv.1	0·10	−23·8	−0·3	0·40	−22·9	3·1	1·13	2·36	0·44	0·97

The temporal correction factor, τ, and the relative stroke plane angles were calculated for the downstroke, β_{rD}, and the upstroke, β_{rU}, assuming either equal support by the two strokes, or support by one stroke only (the downstroke for all sequences except Cv.1).

The estimate for the quasi-steady life coefficients, C_{LD} and C_{LU}, and the rotational coefficients, γ_D and γ_U are also shown.

Ellington's formula (1984*f*, equation 12). It is estimated that the aerodynamic force produced by flies is 4 % less than that which would be produced by a wing executing simple harmonic motion. Hence Ellington's $(d\hat{\phi}/dt)^2$ equals $0{\cdot}96 \times 2\pi$. This is the average value found for flies by Ellington (1984*c*). An error of at most 3 % will be caused by this assumption. This approximation results in the formula:

$$C_L = \frac{4p_w \hat{L}\cos^2\beta_r}{0{\cdot}96\Phi^2\rho\pi^2 n^2 R^2 \hat{r}_2{}^2(s)\cos^2\beta}, \qquad (14)$$

where $\hat{L}$ is the mean lift for each half-stroke divided by the weight. Therefore, if there is equal weight support on the two strokes $\hat{L}$ is 1, whereas for weight support by only one stroke it is 2.

To hover, however, there must be no net horizontal force. The wing drag has little effect on the vertical force produced, since it is much smaller than the lift and because the wings move largely horizontally, but may strongly affect the horizontal force balance. The drag force acting on aerofoils in unsteady flow is unknown. During his analysis of the inclined stroke plane hovering of *Episyrphus*, Ellington gave the maximum possible value of the profile drag coefficient ($C_{Dpro} = 1{\cdot}2$) to the downstroke, despite its low angle of attack. Since the lift coefficient during the downstroke was 5·08, the profile drag coefficient was $0{\cdot}24C_L$. Here the assumption is made that the ratio of lift to drag remains constant. Hence, during horizontal stroke plane hovering, downstroke drag, like lift, will equal that produced during the upstroke. Drag will not affect the force balance in

horizontal stroke plane hovering, but it will do so when the plane is inclined and the upstroke and downstroke lifts are unequal. This is the case in all the sequences in this study. For all of them the Reynolds number was around 1500, so the ratio used by Ellington $C_{Dpro} = 0{\cdot}24C_L$ is used throughout. The minimum drag coefficient of the wing cannot be less than the minimum value for a flat plate (around 0·2 at Reynolds numbers of about 1500) (Ellington, 1984*f*). This minimum value is used when the lift coefficient is lower than 0·8.

Assuming that drag is a fraction of lift, the coefficients can readily be calculated for inclined stroke plane hovering and the relative weight support of the two strokes can be calculated. The lift produced by the wings must balance the insect's weight and there must be no net horizontal force. Two simultaneous equations are set up:

$$C_{LD}\cos\beta_{rD} + C_{LU}\cos\beta_{rU} = 2C_{Lhor}\,, \tag{15a}$$

$$C_{LD}\sin\beta_{rD} + C_{LU}\sin\beta_{rU} - 0{\cdot}24(C_{LD}\cos\beta_{rD}) + 0{\cdot}24(C_{LU}\cos\beta_{rU}) = 0\,, \tag{15b}$$

where the lift coefficient for horizontal stroke plane hovering, C_{Lhor}, is calculated from equation 14.

Since all the hovering sequences showed a noticeably inclined stroke plane, the estimates for the relative stroke plane angles used are those calculated assuming weight support on only one stroke. As these differed by at most 6°, even from the values for equal support, this assumption will not cause large errors in the calculated lift coefficients. The results for all the hovering sequences are given in Table 5.

Calculation of rotational coefficients

Ellington's (1984*c*,*d*) deliberations suggested that the circulation might be created at the beginning of each half-stroke by rotational mechanisms and then remain bound to the wing for the rest of the stroke. Such a circulation should be proportional to ωc^2 for each wing element. He derived a rotational coefficient γ relating the circulation of each element to the mean rotational velocity of stroke reversal $\bar{\omega}$ whereby:

$$\Gamma = \gamma\bar{\omega}c^2\,. \tag{16}$$

If the relative support of the two strokes has been calculated using the quasi-steady analysis, the mean rotational coefficient may be calculated using the expanded form of Ellington's (1984*f*) equation 18:

$$\hat{\gamma} = \frac{\hat{L}mgAR^2\cos\beta_r}{16\rho\hat{\omega}n^2\Phi R^4\hat{v}\hat{r}_1(v)\cos\beta}\,, \tag{17}$$

where $\hat{L}$ is the relative weight support for each half-stroke given as a fraction of the insect's weight so that $\hat{L}_D + \hat{L}_U = 2$.

$\hat{\gamma}$ can be compared with the maximum values expected for postulated rotational mechanisms (such as clap-and-fling and flex) in just the same way that lift

coefficients may be compared with the maximum values for aerofoils in steady flow. The results for the hovering sequences are given in Table 5.

Forward flight

Forward flight is more difficult to analyse than hovering because of the extra complication of the movement of the body, which must be added to that of the wings. If the quasi-steady assumption is made, it is necessary to perform a lengthy integration of the forces produced by each wing section through all stages of the wing beat. It is not possible to use average velocities because of the dependence of aerodynamic force on the second power of the velocity. Further difficulties are added by our ignorance of the pattern of induced velocity in these unsteady conditions, and the aerodynamic force produced must also overcome the parasite drag of the body. Dudley's (1987) lengthy analysis of forward flight showed that the quasi-steady assumption is untenable in this situation. Unsteady effects must be important. I therefore outline below a novel means of analysing forward flight based on vortex theory.

As we have seen, it is probable that the circulation around the wings during each half-stroke is created by rotational mechanisms at stroke reversal and stays attached until the end of the stroke. The wing rotates at approximately the same angular velocity during both pronation and supination, so an equal, but opposite, circulation should be created for each stroke. To test whether this actually happens, the analysis calculates the direction of the aerodynamic force that would result. This direction is then compared with that needed to both support and propel the animal through the air. If the two directions are significantly different, it is clear the assumptions of the model are not valid.

The equal but opposite circulation model

If equal, but opposite, circulations are created by wing rotation at the ends of each half-stroke, the lift created by the motion of a wing section will be proportional to the first power of its velocity:

$$L = \rho\Gamma U \tag{18}$$

(as opposed to the dependence of lift on the square of velocity, if the circulation is produced by translation).

The lift may be simply calculated, therefore, as the wing velocity can be averaged over time. Little is known of the way drag varies during unsteady flow (Ellington, 1984*f*), but it is clear from Ellington's analysis of inclined stroke plane hovering that it cannot be estimated by quasi-steady theory. In this analysis I make the assumption that drag may be estimated as a constant fraction of the lift:

$$D = \rho\Gamma U/K\,. \tag{19}$$

The assumption seems to be a reasonable one since, in the analysis of hovering, a similar assumption was necessary before a balance of forces could be achieved. Furthermore, an aerofoil would be expected to work at its optimal lift-to-drag

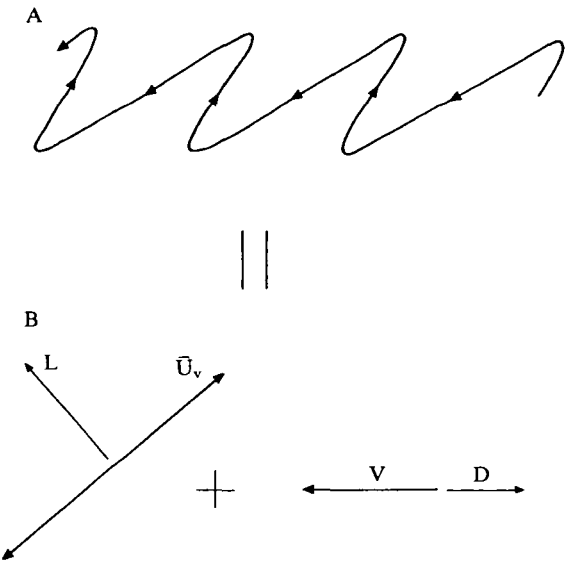

Fig. 9. The model for the analysis of forward flight. Wing motion (A) is the sum (B) of flapping and body velocity. If circulation is set up by wing rotation at stroke reversal, aerodynamic forces will be proportional to the first power of the velocity (V). Here the circulation is of equal strength, but in opposite directions for each stroke. The resultant force can therefore be found by vector addition of the lift due to flapping (L) and the drag due to body velocity (D). $\bar{U}_v$ is the average flapping velocity.

ratio. This assumption has the benefit of greatly simplifying the mathematics, since all terms will vary with the first power of wing velocity and may be averaged over time. Optimal lift-to-drag ratios may be estimated from the results obtained in steady flow on real aerofoils to find the constant K. The drag of real wings includes a component of induced drag, so in this analysis the induced velocity distribution need not be explicitly calculated.

When the body of an insect is still and its wings are moving along a stroke plane, each stroke producing equal lift, the resultant force produced will be at right angles to the stroke plane or 'actuator disc' (Vogel, 1966; Ellington, 1984*c*). If the body is moving as well, however, the two strokes will produce unequal forces because the relative velocity of the wings during the two strokes will be different. Each point on the wing will follow a saw-tooth pattern (Fig. 9A), the shape of which will vary along the wing length. The resultant force produced will no longer be at right angles to the stroke plane, but be angled back.

The velocity of a wing section is the vector sum of its flapping velocity and the body velocity (Fig. 9B) and since the aerodynamic forces are assumed to be proportional to velocity, they can be calculated by summing the forces produced by the two motions. Two net forces will result. The wing-flapping motion will produce lift at right angles to the stroke plane (Fig. 9B). The drag produced by the flapping motion during the two strokes will, however, be equal and opposite, so no

net drag force will result in the stroke plane. The movement of the wings at the velocity of the body will result in drag opposing body motion (Fig. 9B). Lift will also result from this motion, but will be of opposite sign during the two strokes, since the circulation will be reversed, so no net force will result normal to the body velocity.

The resultant force can be simply found by vector addition of the two net forces. The magnitude of these forces will vary along the wing as the local circulation and flapping velocity change. The circulation produced by rotation of a wing chord is $\Gamma = k\omega c^2$, where c is the local value of the wing chord. If the wing rotates as a flat plate, the local value of circulation will be proportional to the square of the chord length, like the local value of the virtual mass. The centre of lift production is therefore at the centre of virtual mass, a distance $\hat{r}_1(v)R$ from the wing base. The average flapping velocity $\bar{V}_f$ of the wing is taken at this point:

$$\bar{V}_f = 2\Phi n R \hat{r}_1(v) , \tag{20}$$

and a new advance ratio, J_R, can be calculated:

$$J_R = \hat{V}/2\Phi\hat{r}_1(v) . \tag{21}$$

The relative values of the lift produced by the flapping velocity and the drag produced by the body velocity will depend on this advance ratio and on the lift-to-drag coefficient K of the aerofoil at the appropriate Reynolds number, so:

$$\begin{aligned} D/L &= J_R/K , \\ &= \hat{V}/2K\Phi\hat{r}_1(v) . \end{aligned} \tag{22}$$

In tests on real insect wings, Nachtigall (1977) obtained a maximum lift-to-drag ratio of 3·8 for *Tipula* wings at a Reynolds number of 1500, and Vogel (1967) obtained a ratio of 1·8 for *Drosophila* wings at a Reynolds number of 200. Values of K are calculated for the forward flight sequences using Ellington's estimate of the Reynolds number:

$$Re = 4\Phi n R^2/\nu \mathcal{A} R , \tag{23}$$

where ν is the kinematic viscosity of air, and assuming that intermediate values of K can be estimated by interpolation between these experimental values, so that:

$$K = 0{\cdot}30 Re^{0{\cdot}344} . \tag{24}$$

In our present state of ignorance of the drag forces during unsteady flow, this is the most realistic estimate that I can make.

The angle of the resultant force, ψ_C, from vertical is then found by vector addition of the lift and drag terms.

The resultant force produced by the wings must support the weight of the insect and overcome the parasite drag of the body. In insects, parasite drag has been found to be but a small fraction of body weight (Weis-Fogh, 1956; Vogel, 1966; Dudley, 1987), and so the force vector should point only slightly forwards. Vogel (1967) found that the parasite drags of the bodies of *Drosophila* were 0·07 mg and 0·18 mg at 1 and 2 $m\,s^{-1}$, respectively. At these speeds the force vectors would

Table 6. *Equal circulation estimates of force vectors in forward flight sequences*

Sequence	β (degrees)	J_R	*Re*	K	ψ_C (degrees)	ψ_A (degrees)
Et.3b	12·1	0·23	1451	3·79	8·7	*
Bm.1b	10·2	0·27	1234	3·59	7·1	*
Bm.2	5·9	0·32	1019	3·36	3·6	*
Cv.2	−16·2	0·31	1360	3·73	−20·6	0·9
Cv.3	20·0	0·15	1130	3·49	19·6	0·3
Cv.4	47·1	0·67	1540	3·88	33·4	2·6
Dm.1	−10·9	0·32	103	1·53	−17·3	1·5
Dm.2	31·0	0·64	110	1·56	4·9	3·3
Sm.1	14·0	1·13	254	2·09	−8·1	6·3
Cs.1	7·2	0·14	724	3·00	5·2	0·4
Tp.1	31·2	0·22	748	3·03	29·7	*

The stroke plane angle, β, the rotational advance ratio, J_R, and the Reynolds number, *Re*, for each forward flight sequence and the lift-to-drag ratio, K, which results.

The inclination of the force vector, ψ_C, calculated assuming equal but opposite circulations, is shown, alongside the approximate inclination of the force vector needed to support and propel the insect, ψ_A.

An asterisk denotes that the insect is accelerating, so the inclination required is unknown.

have to be inclined forward by 4° and 10°, respectively. The parasite drag for my *Drosophila* and *Simulium* sequences has been estimated from these results. Dudley (1987) found that the drag of the bodies of *Eristalis* was around 0·02 mg at $1\,m\,s^{-1}$ and 0·05 mg at $2\,m\,s^{-1}$. For the remaining insects in this study (all of which are about the same size as *Eristalis*) the parasite drag has been estimated from these results. The lift-to-drag ratios of insect bodies are less than 0·5 (Dudley, 1987), so the lift produced by the insects in flight can be ignored. The angles of inclination of the force vectors, ψ_A, necessary to overcome drag are given in Table 6.

Differences between the angles ψ_C and ψ_A will reveal a departure from the equal circulation model. If more circulation were built up for the downstroke than for the upstroke, more drag would result and the force vector would point further backwards; the net force produced would therefore point further back than the model would estimate. The reverse would be the case if more circulation were built up for the upstroke. Values from the analysis of forward flights are given in Table 6.

Results of analysis

Eristalis tenax

Eristalis hovered with a stroke plane inclined at about 13° in the flight cage and in the four hovering sequences it was calculated that the downstroke provided

roughly twice the weight support of the upstroke. The lift coefficients for the downstroke, ranging from 2·21 to 2·61, are well above the theoretical limit at a Reynolds number of around 1500, so the magnitude of the force is beyond explanation by quasi-steady analysis. The direction of the aerodynamic force cannot be accounted for by quasi-steady effects, since the angles of attack are similar for the two strokes and they should therefore produce similar values of lift. This would result in a forward-inclined force.

The unequal weight support may be caused by the timing of pronation and supination. In these hovering sequences, pronation was delayed until after the start of the downstroke, whereas supination was slightly brought forward. If the circulation for each stroke was created by Ellington's flex mechanism, delayed pronation would help create greater lift during the downstroke, and advanced supination would reduce upstroke lift. This is exactly what happens, providing evidence to support Ellington's mechanism. The rotational lift coefficients are all below 1 and within the possible range of this rotational mechanism.

The kinematics of the hovering Et.1 proved to be very variable. The stroke amplitude varied by up to 14°, and as this rose the wing beat frequency tended to fall. As a result, the average velocity of the wing, and hence the magnitude of the lift coefficients required, did not vary much. The main effect of varying the stroke amplitude would be to change the induced downwash w_o past the stroke plane. With a lower amplitude the downwash velocity would be greater and this would change the inclination of the relative velocity. The lift produced by the downstroke would point further back, whereas that produced by the upstroke would point further forward. During inclined stroke plane hovering the downstroke provides more lift than the upstroke so the net result would be to incline the force vector backwards. In the aerodynamic analysis of the hovering Et.1 it was assumed that the forces were always balanced and that the net aerodynamic force was always vertical. It was therefore assumed that the relative support of the two strokes had changed between the sequences. This might not have been the case. Instead, the relative support may have stayed the same and the stroke amplitude may have been under constant control to provide transient minor accelerations which would adjust the position of the insect.

In the two sequences of Et.3, the insect first hovered (Et.3a) and then turned and accelerated out of the film frame. (Et.3b) is a sequence taken as the insect was accelerating. The stroke plane angle, β, is actually reduced slightly, from 13·7° to 12·1°, so the insect is clearly not manoeuvring like a helicopter, which would require an increase in β of over 10°. Neither is it using its wings to produce drag, since the angles of attack are the same for the two strokes. Only two differences in kinematics are noticeable: (i) the amplitude of the wing beat is greater in the second sequence; (ii) pronation and supination are more symmetrical about the ends of the beat in the second sequence. In particular, mid pronation occurs nearer the very top of the beat.

As a result of (ii) a more equal circulation should now be produced on both strokes and this should incline the force vector forwards, resulting in the observed

acceleration. Merely by altering the timing of stroke reversal the insect can manoeuvre sharply.

Bibio marci

Bibio was filmed in take-off and then in rising flight. Just after take-off, the stroke plane of the female Bm.1 was inclined at 30° to the horizontal and the wing beat amplitude was high (Bm.1a). The quasi-steady analysis of the beat made it clear that even if the upstroke produced no lift the animal must have been accelerating forwards by around $0{\cdot}1\,\boldsymbol{g}$. It was assumed that no lift was being produced by the upstroke, since little acceleration was evident and any upstroke lift would have caused extremely high forward accelerations. It is clear that the downstroke lift coefficient, 4·42, was far too high to be produced by a quasi-steady mechanism. In this sequence the wings were meeting at the top of the beat and performing the kinematics of the clap-and-fling mechanism and it is likely that circulation was being produced by this mechanism. Previous authors have found that animals using this clap-and-fling mechanism can produce lift coefficients in excess of 5 (Weis-Fogh, 1973; U. M. Norberg, 1975, 1976) and the rotational coefficient, γ, of 1·55 is below the theoretical maximum for a fling or peel (Ellington, 1984*d*). Supination of the wings is advanced and this may help to shed the high circulation at the end of the downstroke without building up an upstroke circulation.

Later on in its flight, when the animal is moving and accelerating forwards and upwards (Bm.1b), the stroke plane is actually at the much lower angle of 10°. The sequence of the male (Bm.2), shows the insect at a similar velocity with a stroke plane angle of 6°. In both these cases, the circulation on the two strokes must be similar, as the equal circulation estimate of the direction of the force vector, ψ_C, points only slightly forwards. Two differences in the kinematics might explain this: (i) the wings no longer meet at the top of the upstroke and (ii) supination occurs later, at the very bottom of the downstroke.

Less circulation will be built up on the downstroke since clap-and-fling no longer occurs, whereas more circulation will be built up by the flex mechanism for the upstroke. Varying the extent of clap-and-fling may be another mechanism for changing the direction of the force vector and hence manoeuvring quickly.

Calliphora vicina

Bluebottles rarely seem to hover and only one sequence of hovering (Cv.1) was obtained. The animal has a near vertical body and a *negatively* inclined stroke plane. To produce a net vertical force, therefore, it must be producing more lift (and hence drag) on the upstroke. The lift coefficient calculated for the upstroke, 2·36, is well above the value possible by a quasi-steady mechanism.

The sequences Cv.2 and Cv.3 show animals in rising forward flight. In Cv.2 the stroke plane angle is negative. If there were equal circulation during each half-stroke the wings would produce a force angled 20° back. Since the animal was travelling upwards and forwards, the upstroke must have been producing greater

lift (and hence drag) than the downstroke. In Cv.3, however, the stroke plane is at a positive angle of 20° and the downstroke in this case seems to be the more effective. The stroke amplitudes are similar and again the only difference seems to lie in the kinematics of stroke reversal. In Cv.2 supination is delayed until after stroke reversal and is noticeably faster than pronation. In Cv.3 pronation is delayed. We have already seen that delay in rotation should help to build up a higher circulation for the coming stroke, so these differences could be responsible for the difference in the relative lift production.

The delay in supination seems to be correlated with the extent of ventral flexion along the transverse flexion line of *Calliphora*. While it is flexing, the wing does not seem to rotate, which seems to imply that the torsional axis of the wing is shifted backwards. The greater flexion which occurs in both Cv.1 and Cv.2 is followed by the fast recoil of the leading edge, resulting in fast, late supination. The wing tip rises at this point in these sequences, which may reflect strong lift generation.

The fast forward flight sequence Cv.4 shows an insect with a strongly inclined stroke plane. It is probably using the downstroke much more than the upstroke. The wings are approaching clap-and-fling dorsally.

Varying the extent of ventral flexion, the dorsal extent of the wing beat and the timing of stroke reversal may all help change the force vector produced by the wings and help in manoeuvres.

Drosophila melanogaster

Ventral flexion of the wing also occurs in *Drosophila* and was observed in both the sequence shown. In the rising flight sequence Dm.1, the stroke plane is negatively inclined so the upstroke is clearly providing more force. In the fast forward flight sequence Dm.2, the stroke plane is inclined forwards and seems to be consistent with the equal circulation model. *Drosophila*, too, seems to be able to control the force vector independently of the stroke plane to some extent. In the films, the insects seldom used the clap-and-fling mechanism, unlike the tethered flies of Vogel (1966).

Simulium

The low stroke plane angle of *Simulium* in forward flight (Sm.1) suggests that the upstroke circulation was greater than that of the downstroke. The wings of this animal clearly bent ventrally along its transverse flexion line at the end of the downstroke, and then recoiled to supinate quickly, which should produce a large upstroke circulation.

Conops strigatus

The only sequence of *Conops* is of slow forward flight. The stroke plane is consistent with equal circulation on both strokes and the wing shows no sign of bending.

Tipula paludosa

In the only sequence of film of a crane fly the animal is accelerating forwards with a suitably inclined stroke plane. The wings perform a clap-and-fling dorsally which may imply a higher downstroke circulation.

Discussion

It is clear that the quasi-steady analysis of lift production is incapable of explaining the magnitude and direction of the forces produced by many flies. As we have also seen, a model in which there is an equal circulation on each stroke often wrongly predicts the direction of the force vector. The flies did not manoeuvre like helicopters, but seemed, like the muscids studied by Wagner (1986), to be capable of tilting the force vector without having to tilt the stroke plane, by changing the relative lift produced by the upstroke and downstroke.

This independent fore–aft control of the force vector was not observed by Vogel (1966) or David (1978) in the steady flight of *Drosophila*. Instead, they found that the flight velocity was closely correlated with the stroke plane angle: results consistent with a helicopter-like control system, using a tilting actuator disc.

The differences were probably caused by the different experimental conditions. The flies studied by Wagner and me were manoeuvring freely. Independent control of the force vector is probably used to speed up manoeuvres which would otherwise require the body axis to be tilted, and would therefore be rather sluggish (Ellington, 1984*c*). Once flying at the desired velocity, the body angle could then be adjusted to a value which would result in the most economical flight.

The main method by which the force vector may be independently controlled seems to be by changing the exact timing of pronation and supination, as described by Ellington (1984*c*,*d*). Delaying rotation until after the end of a stroke seems to help build up an increased circulation, whereas advancing rotation seems to reduce the circulation for the coming half-stroke. In the insects that possess a ventral flexion mechanism, it appears that the upstroke circulation may be increased when the wing bends ventrally at the end of the downstroke. This may be because, as the wing straightens again, supination may be speeded up and delayed. In many insects, an increased downstroke circulation may be built up using the clap-and-fling mechanism.

It is unfortunate that there is currently no reliable method of accurately measuring the angle of attack of the wings of insects in free flight. The timing and speed of rotation can therefore only be estimated. Experimental tests are clearly needed to verify Ellington's rotational flex mechanism, and to establish the exact effect of the timing and speed of rotation.

Aerodynamic mechanisms and flight behaviour in the field

The methods by which different flies change the force vector and hence manoeuvre are different and are related to the needs of the insects in the wild.

In the field, *Eristalis* can hover with either an inclined or a horizontal stroke

plane. Males frequently hover with an inclined plane in a patch of sunlight until a flying object passes by. Collett & Land (1978) found that they then compute an interception course and accelerate along it at up to $30\,m\,s^{-2}$. They reasoned that males would eventually overtake the object if it was a female *Eristalis* travelling at $8\,m\,s^{-1}$, a speed which they presumed to be the cruising speed of the species. Presumably, they would then attempt to mate.

Clearly, the faster the males accelerate, the more likely is a chase to be successful. Using an inclined stroke plane enables an animal to accelerate forwards extremely quickly. During hovering we have seen that lift production is limited largely to the downstroke and a vertical resultant force is produced. By changing the timing of wing rotation, both wing strokes can be made to produce lift and the resultant force can be tilted forwards, almost instantaneously, to point at right angles to the stroke plane. The insect can accelerate without needing to tilt its body. The acceleration may be further increased by raising the wing beat amplitude. The more inclined the stroke plane and the smaller the initial amplitude of the beat, therefore, the faster an insect will be able to accelerate. An insect hovering with an inclined stroke plane may be akin to a sprinter on starting blocks.

Inclined stroke plane hovering is also extremely precise, and animals using it may remain with the body absolutely stationary, even in turbulent conditions. We have seen that by raising the stroke amplitude and reducing the frequency (or *vice-versa*) the induced velocity can be changed. This changes the relative velocity of the wings, and hence the force vector, produced predominantly by the downstroke, may be tilted. This could provide the fine control of the force vector. It may be for these reasons that flies which hover at flowers, like the Bombyliidae, use an inclined stroke plane (personal observation). Unilateral control of wing beat amplitude can provide control of yaw during hovering, just as it does in other insects (Gotz, 1968).

The female *Eristalis* I have observed tended to hover with a horizontal stroke plane. They probably have less need to accelerate forwards quickly than males and when foraging they tend to land heavily on the flowers on which they feed. Use of a horizontal stroke plane will reduce their energy expenditure (Ellington, 1984*f*), mainly because the induced power requirement is lower, because of the larger stroke plane angle and the lower periodicity of the wake produced.

Both males and females of *Bibio marci* often fly into the wind, keeping their station in a swarm, where the males seize the females. Individuals of neither sex maintain their position precisely and they seem to produce lift using both half-strokes. The exception is at take-off, when the body is horizontal and the stroke plane is therefore inclined. High lift can be created during the downstroke by use of the clap-and-fling mechanism. Early supination at the end of the downstroke can ensure that little or no lift is produced during the upstroke. As a result, a vertical force can be produced, which allows a vertical take-off. The use of the clap-and-fling mechanism seems to be widespread for this manoeuvre.

Calliphora is a most versatile flier, even in the flight cage. Insects were observed

flying freely in all directions, and manoeuvring sharply. The usual method for turns was to bank and then for the inward-pointing force vector to accelerate the insect. In one case an insect in rising flight rolled upside down, accelerated downwards and rolled the right way up to end up in a dive. To achieve the fast roll, insects tended to produce one or two wing beats with a very low amplitude on one side. I have suggested (Ennos, 1987) that these could have been produced by using the rear groove of the pleural wing process to stop the wing. The wing tended to flex noticeably during these low-amplitude beats and this would reduce the stress at the wing articulation. It is possible that such a flexion mechanism is essential before such low-amplitude wing beats can be produced and hence before this ability to roll quickly can be achieved. In studies of the chasing behaviour of calyptrate flies (Collett & Land, 1974; Wagner, 1986) the flies were observed to slow down before turns and to accelerate afterwards. We have seen that by changing the extent and timing of ventral flexion and wing rotation these flies can vary the fore–aft force component considerably. Wagner (1986) also noted that calyptrate flies could vary this vector independently of the stroke plane to some extent. These insects can produce more lift on the upstroke and hence hover with a negatively inclined stroke plane. The ability quickly to alter the direction of the force will help in accelerations and decelerations, and the use of a clap-and-fling mechanism or extra flexion at the end of the downstroke may also provide nose-down or nose-up pitching moments to alter the body angle and speed up these manoeuvres. The capability of ventral flexion might give these insects extra control of the force vector in all planes and lead to their great manoeuvrability. It seems likely that both *Drosophila* and *Simulium*, which possess similar mechanisms, manoeuvre in the same way, and in the field both demonstrate high manoeuvrability.

The Conopidae are apparently capable of very accurate flight since they are known to lay their eggs on bees in flight, but the film is insufficient to suggest how this might be achieved. Field observations suggest that they often use an inclined stroke plane and dart forward, like *Eristalis* males.

Crane flies do not seem to control their flight velocity very accurately as they often hit obstructions in the field and therefore it is unlikely that they use any special method to manoeuvre.

I would like to thank Dr C. P. Ellington and Dr T. R. Dudley for the use of their analysis program, and Dr R. J. Wootton for his help and criticism during the production of the manuscript. The work was carried out while under tenure of an SERC research studentship.

References

Collett, T. S. & Land, M. F. (1974). Chasing behaviour of houseflies (*Fannia canicularis*): a description and analysis. *J. comp. Physiol.* **89**, 331–357.

Collett, T. S. & Land, M. F. (1978). How hoverflies compute interception courses. *J. comp. Physiol.* **125**, 191–204.

DAVID, C. T. (1978). The relationship between body angle and flight speed in free-flying *Drosophila*. *Physiol. Entomol.* **3**, 191–195.

DUDLEY, T. R. (1987). The mechanics of forward flight in insects. PhD thesis, University of Cambridge.

ELLINGTON, C. P. (1978). The aerodynamics of normal hovering flight: three approaches. In *Comparative Physiology – Water, Ions and Fluid Mechanics* (ed. K. Schmidt-Nielsen, L. Bolis & S. H. P. Maddrell), pp. 327–345. Cambridge: Cambridge University Press.

ELLINGTON, C. P. (1980). Vortices and hovering flight. In *Instationäre Effekte an Schwingenden Tierflügeln* (ed. W. Nachtigall), pp. 64–101. Wiesbaden: Franz Steiner.

ELLINGTON, C. P. (1984*a*). The aerodynamics of hovering insect flight. I. The quasi-steady analysis. *Phil. Trans. R. Soc. Ser.* B **305**, 1–15.

ELLINGTON, C. P. (1984*b*). The aerodynamics of hovering insect flight. II. Morphological parameters. *Phil. Trans. R. Soc. Ser.* B **305**, 17–40.

ELLINGTON, C. P. (1984*c*). The aerodynamics of hovering insect flight. III. Kinematics. *Phil. Trans. R. Soc. Ser.* B **305**, 41–78.

ELLINGTON, C. P. (1984*d*). The aerodynamics of hovering insect flight. IV. Aerodynamic mechanisms. *Phil. Trans. R. Soc. Ser.* B **305**, 79–113.

ELLINGTON, C. P. (1984*e*). The aerodynamics of hovering insect flight. V. A vortex theory. *Phil. Trans. R. Soc. Ser.* B **305**, 115–144.

ELLINGTON, C. P. (1984*f*). The aerodynamics of hovering insect flight. VI. Lift and power requirements. *Phil. Trans. R. Soc. Ser.* B **305**, 145–181.

ENNOS, A. R. (1987). A comparative study of the flight mechanism of Diptera. *J. exp. Biol.* **127**, 355–372.

ENNOS, A. R. (1988). The importance of torsion in the design of insect wings. *J. exp. Biol.* **140**, 137–160.

ENNOS, A. R. (1989). A comparative study of the functional morphology of the wings of some Diptera. *J. Linn. Soc. (Zool.)* (in press).

GOTZ, K. G. (1968). Flight control in *Drosophila* by visual perception of motion. *Kybernetic* **4**, 199–208.

LIGHTHILL, M. J. (1973). On the Weis-Fogh mechanism of lift generation. *J. Fluid Mech.* **60**, 1–17.

MAXWORTHY, T. (1979). Experiments on the Weis-Fogh mechanism of lift generation by insects in hovering flight. I. Dynamics of the 'fling'. *J. Fluid Mech.* **93**, 47–63.

NACHTIGALL, W. (1966). Die Kinematik der Schlagflügelbewegungen von Dipteren. Methodische und Analytische Grundlagen zur Biophysik des Insektenflugs. *Z. vergl. Physiol.* **52**, 155–211.

NACHTIGALL, W. (1977). Die aerodynamische Polare des Tipula-Flügels und eine Einrichtung zur halbautomatischen Polarenaufnahme. In *The Physiology of Movement; Biomechanics* (ed. W. Nachtigall), pp. 347–352. Stuttgart: Fischer.

NACHTIGALL, W. (1979). Rasche Richtungsänderungen und Torsionen schwingender Fliegenflügel und Hypothesen über zugeordnete instationäre Strömungseffekte. *J. comp. Physiol.* **133**, 351–355.

NACHTIGALL, W. (1981). Insect flight aerodynamics. In *Locomotion and Energetics in Arthropods* (ed. C. F. Herreid & C. R. Fourtner), pp. 127–162. New York: Plenum Press.

NEWMAN, D. J. S. (1982). The functional wing morphology of some Odonata. PhD thesis, University of Exeter.

NORBERG, R. Å. (1975). Hovering flight of the dragonfly *Aeschna juncea* L., kinematics and aerodynamics. In *Swimming and Flying in Nature*, vol. 2 (ed. T. Y. Wu, C. J. Brokaw & C. Brennen), pp. 763–781. New York: Plenum Press.

NORBERG, U. M. (1975). Hovering flight of the pied flycatcher (*Ficedula hypoleuca*). In *Swimming and Flying in Nature*, vol. 2 (ed. T. Y. Wu, C. J. Brokaw & C. Brennen), pp. 869–881. New York: Plenum Press.

NORBERG, U. M. (1976). Aerodynamics, kinematics and energetics of horizontal flight in the long-eared bat *Plecotus auritus*. *J. exp. Biol.* **65**, 179–212.

OSBORNE, M. F. M. (1951). Aerodynamics of flapping flight with application to insects. *J. exp. Biol.* **28**, 221–245.

VOGEL, S. (1966). Flight in *Drosophila*. I. Flight performance of tethered flies. *J. exp. Biol.* **44**, 567–578.

VOGEL, S. (1967). Flight in *Drosophila*. III. Aerodynamic characteristics of fly wings and wing models. *J. exp. Biol.* **46**, 431–443.

WAGNER, H. (1925). Uber die Entstehung des dynamischen Auftriebes von Tragflugeln. *Z. angew. Math. Mech.* **5**, 17–35.

WAGNER, H. (1986). Flight performance and visual control of flight of the free-flying housefly (*Musca domestica* L.). *Phil. Trans. R. Soc. Ser.* B **312**, 527–600.

WEIS-FOGH, T. (1956). Biology and physics of locust flight. II. Flight performance of the desert locust (*Schistocerca gregaria*). *Phil. Trans. R. Soc. Ser.* B **239**, 459–510.

WEIS-FOGH, T. (1972). Energetics of hovering flight in hummingbirds and in *Drosophila*. *J. exp. Biol.* **56**, 79–104.

WEIS-FOGH, T. (1973). Quick estimates of flight fitness in hovering animals, including novel mechanisms for lift production. *J. exp. Biol.* **59**, 169–230.

WOOTTON, R. J. (1981). Support and deformability in insect wings. *J. Zool., Lond.* **193**, 447–468.